Environmental Science & Technology

pubs.acs.org/est

Article

Respiratory Vinyl Chloride Reductive Dechlorination to Ethene in TceA-Expressing *Dehalococcoides mccartyi*

Jun Yan,* Jingjing Wang, Manuel I. Villalobos Solis, Huijuan Jin, Karuna Chourey, Xiuying Li, Yi Yang, Yongchao Yin, Robert L. Hettich, and Frank E. Löffler*

Cite This: *Environ. Sci. Technol.* 2021, 55, 4831−4841

Read Online

ACCESS | Metrics & More | Article Recommendations | Supporting Information

ABSTRACT: Bioremediation of chlorinated ethenes in anoxic aquifers hinges on organohalide-respiring *Dehalococcoidia* expressing vinyl chloride (VC) reductive dehalogenase (RDase). The *tceA* gene encoding the trichloroethene-dechlorinating RDase TceA is frequently detected in contaminated groundwater but not recognized as a biomarker for VC detoxification. We demonstrate that *tceA*-carrying *Dehalococcoides mccartyi* (*Dhc*) strains FL2 and 195 grow with VC as an electron acceptor when sufficient vitamin B_{12} (B_{12}) is provided. Strain FL2 cultures that received 50 $\mu g\ L^{-1}$ B_{12} completely dechlorinated VC to ethene at rates of 14.80 ± 1.30 $\mu M\ day^{-1}$ and attained 1.64 ± 0.11 × 10^8 cells per μmol of VC consumed. Strain 195 attained similar growth yields of 1.80 ± 1.00 × 10^8 cells per μmol of VC consumed, and both strains could be consecutively transferred with VC as the electron acceptor. Proteomic analysis demonstrated TceA expression in VC-grown strain FL2 cultures. Resequencing of the strain FL2 and strain 195 *tceA* genes identified non-synonymous substitutions, although their consequences for TceA function are currently unknown. The finding that *Dhc* strains expressing TceA respire VC can explain ethene formation at chlorinated solvent sites, where quantitative polymerase chain reaction analysis indicates that *tceA* dominates the RDase gene pool.

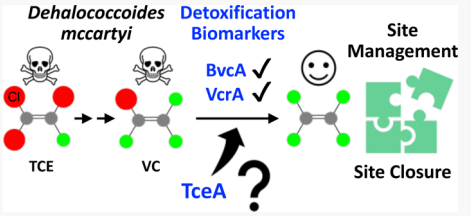

Downloaded via Frank Loeffler on May 3, 2021 at 19:56:47 (UTC).
See https://pubs.acs.org/sharingguidelines for options on how to legitimately share published articles.

INTRODUCTION

Taxonomically diverse organohalide-respiring bacteria (OHRB) utilize organohalides as electron acceptors in energy-conserving reductive dechlorination reactions.[1] A unifying feature of the organohalide respiratory chain is the involvement of reductive dehalogenases (RDases) as the terminal reductases, which determine the range of halogenated substrates the OHRB can utilize.[2,3] Biochemically characterized RDases are membrane-associated iron−sulfur proteins that harbor a corrinoid prosthetic group [i.e., vitamin B_{12} (B_{12}) derivatives] to cleave carbon−halogen bonds.[2,4] OHRB access corrinoids via *de novo* biosynthesis[5] or uptake of complete cobamides or precursors generated by corrinoid-producing members of the microbial community[6−8] to assemble functional RDases required for the organisms' energy metabolism.

OHRB play relevant roles in the cycling of naturally produced organohalides and are the foundation for productive bioremediation of anthropogenic chlorinated solvents such as tetrachloroethene (PCE) and trichloroethene (TCE).[9−11] While diverse OHRB harboring functionally equivalent RDases dechlorinate PCE and TCE to predominantly *cis*-1,2-dichloroethene (*c*DCE), the complete detoxification of dichloroethenes (DCEs) to environmentally benign ethene is exclusively attributed to a subset of OHRB within the class *Dehalococcoidia*.[12,13] Of concern for bioremediation practice is the incomplete dechlorination of DCEs, leading to the formation of vinyl chloride (VC),[14] a human carcinogen.[15]

Dehalococcoides mccartyi (*Dhc*) strains that express BvcA and VcrA RDases utilize DCEs and VC as electron acceptors and dechlorinate these toxins to environmentally benign ethene.[16−18] Recent efforts identified CerA, a novel RDase responsible for growth-linked reductive dechlorination of 1,1-dichloroethene (1,1-DCE) and VC to ethene in "*Candidatus* Dehalogenimonas etheniformans" strain GP, an organism affiliated with the class *Dehalococcoidia* but distant from *Dhc*.[13] Some *Dhc* strains express TceA,[19−21] an RDase that is phylogenetically related with the confirmed VC RDases as well as TdrA, a *trans*-1,2-DCE-to-VC dechlorinating RDase identified in *Dehalogenimonas* sp. strain WBC-2 (Figure 1).[22] TceA dechlorinates TCE, *c*DCE, and 1,1-DCE to VC and can produce ethene, albeit at orders of magnitude lower rates compared to dechlorination of polychlorinated ethenes.[19] Consistent with biochemical studies, *Dhc* strain FL2 and strain 195, which possess the *tceA* gene but lack any of the known VC RDase genes, utilize TCE, *c*DCE, and 1,1-DCE as electron acceptors; however, VC dechlorination to ethene has been reported to be slow, incomplete, and co-metabolic (i.e., only occurred in the presence of a growth-supporting

Received: November 10, 2020
Revised: February 21, 2021
Accepted: February 22, 2021
Published: March 8, 2021

ACS Publications

© 2021 American Chemical Society

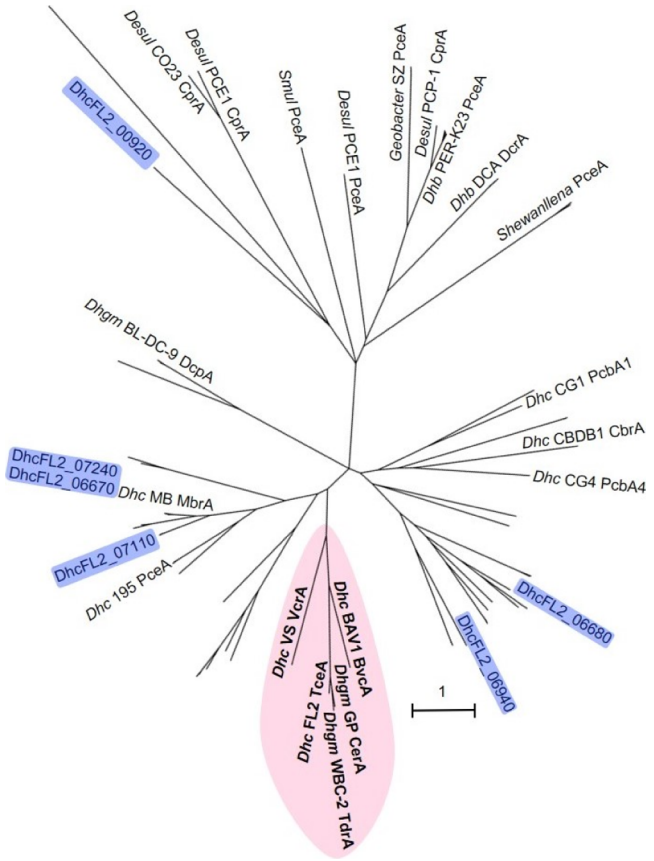

Figure 1. Phylogenetic tree based on protein sequences of 40 RDases with functions assigned by biochemical characterization, expression analysis, or phylogenetic inference from diverse OHRB. Included in the tree are 39 putative RDases encoded on the genomes of *Dhc* strain FL2 and strain 195. RDases with 85% or greater amino acid identity are collapsed and labeled with a single RDase designation. TceA and TdrA cluster together with the known VC RDases BvcA, VcrA, and CerA, as shown in the red highlighted area. Branches representing putative *Dhc* RDases are not labeled except the six putative RDases expressed in *Dhc* strain FL2 during growth with VC (labeled with corresponding locus tag numbers and highlighted in blue color). The scale bar corresponds to one estimated amino acid substitution per site. The tree branches were calculated on the basis of 100 bootstrap iterations.

polychlorinated ethene).[20,23] Therefore, *tceA*-carrying *Dhc* strains are recognized as potential VC producers rather than VC dechlorinators.[12,20]

The implementation of bioremediation at sites impacted with chlorinated contaminants depends on native or augmented OHRB and has emerged as a robust treatment technology.[10,11,24,25] Several studies have correlated the abundance of *Dhc* biomarker genes in groundwater with ethene formation,[24,26] and substantial ethene formation can generally be expected when the *Dhc* cell numbers exceed 10^7 L^{-1}.[24,27,28] Interestingly, the *tceA* gene was found in 50% of groundwater samples in which ethene was detected, and ethene formation occurred at locations where *tceA* was the predominant RDase gene.[24] Field data link *tceA* gene presence and abundance with *in situ* ethene formation; however, this observation cannot be explained with the current understanding of the physiology of *Dhc* strains carrying *tceA*.

To reconcile laboratory experimental results with field observations, we re-investigated the ability of *tceA*-carrying *Dhc* strains to grow with VC as the electron acceptor. An integrated experimental approach that combined physiological studies, growth yield and rate measurements, B_{12} analysis, and proteomic workflows demonstrated that TceA is a VC RDase, but respiratory growth of the *tceA*-carrying *Dhc* strain FL2 and strain 195 with VC is sensitive to B_{12} availability. These findings expand our understanding of *Dhc* ecophysiology and improve the interpretation of quantitative polymerase chain reaction (qPCR) data collected at sites impacted with chlorinated ethenes.

MATERIALS AND METHODS

Chemicals. TCE, *c*DCE, VC, and ethene with greater than 99.5% purity were purchased from Sigma-Aldrich (St. Louis, MO, USA). B_{12} (cyanocobalamin; ≥96% purity) was purchased from Thermo Scientific (Waltham, MA, USA). Other chemicals used in this study were of reagent grade or higher.

RDase Phylogeny. RDases with known functions from diverse OHRB (Table S1) and the putative RDases (Table S2) encoded on the *Dhc* strain FL2 and strain 195 genomes (GenBank accession numbers CP038470.1 and CP000027.1, respectively) were retrieved. Protein sequences were aligned using the Muscle plug-in in Geneious Prime version 2019.1.1 (Biomatters Inc., Newark, NJ, USA) with 10 iterations.[29] The RDase phylogenetic tree was constructed using the PHMYL maximum likelihood tree builder plug-in in Geneious Prime version 2019.1.1 with 100 bootstraps and the Le and Gascuel substitution model.[30]

***Dhc* Growth and Cell Quantification.** Pure cultures of *Dhc* strain FL2 (ATCC BAA-2098), *Dhc* strain 195 (ATCC BAA-2266), and *Dhc* strain BAV1 (ATCC BAA-2100) were grown, as described.[7] *Dhc* strain FL2 was routinely grown with TCE in medium that received a single or multiple doses of 1 $\mu g\ L^{-1}$ B_{12} and transfers occurred every 4−6 weeks. The starting B_{12} concentration was raised to 25 $\mu g\ L^{-1}$ in 2010 and had been further increased to 50 $\mu g\ L^{-1}$ in 2013. All *Dhc* cultures were grown in 160 mL glass serum bottles filled with 100 mL of bicarbonate-buffered (30 mM, pH 7.3), reduced [0.2 mM Na_2S, 0.2 mM L-cysteine, and 0.5 mM 1,4-dithiothreitol (DTT)] mineral salt medium. Acetate (5 mM) was provided as a carbon source, and the headspace consisted of CO_2/N_2 (20/80, v/v). After autoclaving, all bottles were amended with neat TCE (6 μL, 66 μmol, 0.55 mM aqueous phase concentration) or undiluted VC gas (2 mL, 82 μmol, 0.52 mM aqueous phase concentration) as the electron acceptor and hydrogen (10 mL, 413.2 μmol) as the electron donor. B_{12} was added from a filter-sterilized, anoxic B_{12} stock solution (5 or 50 mg L^{-1}) to achieve initial B_{12} concentrations of 1, 10, 25, or 50 $\mu g\ L^{-1}$. Each bottle received a 3% (v/v) inoculum from a *Dhc* culture previously grown with TCE or VC. To establish VC-dechlorinating strain FL2 cultures, culture suspensions (3 mL) for inoculation were centrifuged at 16,110×*g* for 20 min inside an anoxic chamber (Coy Laboratory, Grass Lake, MI, USA) to minimize B_{12} and ethene carryover. The supernatants were decanted, and the cell pellets were suspended in 1 mL of B_{12}-free medium. Replicate bottles amended with TCE (66 μmol) or VC (82 μmol) and B_{12} (50 $\mu g\ L^{-1}$) without inoculum served as negative controls (NCs). All bottles were incubated statically with the stoppers facing up at 30 °C in the dark. Whenever liquid samples were withdrawn, 1 mL H_2 was added to maintain positive pressure inside the culture bottles. For *Dhc* cell quantification, genomic DNA was

https://dx.doi.org/10.1021/acs.est.0c07354
Environ. Sci. Technol. 2021, 55, 4831−4841

extracted and qPCR targeting the *tceA* gene was performed, as described (see the Supporting Information).[31]

PCR and Sanger Sequencing. Amplicons containing the entire *tceA* gene were obtained with primer set 797F and 2490R (Table S3). All PCR reagents were purchased from Thermo Scientific, and each PCR reaction (25 μL) contained 0.5 μL of DNA template, 2.5 μL of 10 × PCR buffer, 1.5 mM $MgCl_2$, 100 μM each dNTP, 0.5 μM each primer, 0.2 U AmpliTaq DNA polymerase, and UltraPure nuclease-free water (Invitrogen, Carlsbad, CA, USA). The PCR cycle conditions were as follows: an initial denaturation step at 94 °C for 2 min followed by 35 cycles at 94 °C for 30 s, annealing at 54 °C for 45 s, extension at 72 °C for 1 min, and a final extension step at 72 °C for 7 min. PCR products were visualized using agarose (1.5%, w/v) gel electrophoresis, purified using the MO Bio UltraClean PCR clean-up kit (MO BIO, Carlsbad, CA, USA), and quantified using a NanoDrop 2000 spectrophotometer (Thermo Scientific). To assemble the entire *tceA* gene sequence, forward primers 797F and TceA1270F and reverse primers TceA1336R and 2490R were used to amplify the positive-sense and negative-sense strands in Sanger sequencing, which was performed using an Applied Biosystems 3730 Genetic Analyzer (Thermo Scientific) at the University of Tennessee' s Genomics Core. Sequencing chromatograms were visually inspected, and the *tceA* gene sequence was assembled using Geneious Prime version 2019.1.1.

B_{12} Quantification. The reduced form of B_{12} in culture supernatant was reacted with KCN following an established protocol with modifications, as described (see the Supporting Information).[32] B_{12} analysis was performed using a Vanquish UHPLC system in tandem with a Q Exactive Hybrid Quadrupole-Orbitrap mass spectrometer (Thermo Scientific). A 2−10 μL aliquot of each sample was loaded onto a Hypersil GOLD column (Thermo Scientific; 2.6 μm pore size, 2.1 mm inner diameter × 100 mm length) operated at 30 °C. Samples were separated at a flowrate of 0.3 mL min^{-1} using 0.1% (v/v) formic acid (≥96% purity, Sigma-Aldrich) in water as eluent A and acetonitrile (≥99.9% purity, Sigma-Aldrich) as eluent B. The initial mobile phase composition of 95% A and 5% B changed to 85% A and 15% B over 2.8 min, to 75% A and 25% B over 1.7 min, and further to 30% A and 70% B over an additional 1.5 min time period. The mobile phase composition reverted to 95% A and 5% B over a 0.5 min time period followed by a 1.5 min hold for column equilibration. The mass spectrometer was operated in the positive electrospray ionization (ESI+) mode with the sheath gas set at 40 arbitrary units, the auxiliary gas set at 10 arbitrary units, the spay voltage set at 3800 V, and a capillary temperature of 350 °C. Full-scan mass spectra were acquired with a mass range of 100−1500 m/z and a resolution of 70,000. Ion fragmentation was performed after each full scan using a normalized collision energy of 35 eV. MS/MS spectra were acquired in the parallel reaction monitoring mode to capture signature transitions of abundant primary and secondary fragment ions of B_{12} in the full-scan spectrum. Raw mass spectra data were processed and analyzed using the Xcalibur software with default settings. The most abundant primary ion of fragmented B_{12} is the $[M + 2H]^{2+}$ adduct with a m/z value of 678.288, which was further fragmented into secondary ions including adducts with m/z ratios of 147.093, 359.099, and 456.727 (Figure S1). The adduct at m/z 147.093 corresponds to the [5,6-dimethylbenzimidazole (DMB) + H]$^+$ ion and is the dominant fragment among all secondary products. Integrated signal intensity of the $[DMB + H]^+$ adduct exhibits excellent correlation (r^2 = 0.998−0.999) with B_{12} injection amounts and thus was selected for B_{12} quantification (Figure S1). The B_{12} recovery efficiency was 96 ± 8%. Linearity was observed between 0.1 and 100 μg L^{-1} B_{12} (2 μL of injection volume) with a detection limit of 0.05 μg L^{-1} (10 μL of injection volume).

Proteomic Analysis. Following complete dechlorination to ethene, three bottles of VC-fed strain FL2 cultures amended with 50 μg L^{-1} B_{12} were combined for global proteomic analysis. The total volume of combined culture suspension was 300 mL containing about 3.74 × 10^{10} *Dhc* cells. Cells were collected onto a 47 mm diameter 0.22 μm pore size polyethersulfone membrane filter (Pall Life Sciences, Port Washington, NY, USA) via vacuum filtration. The membrane was aseptically cut, and the pieces were transferred to individual 20 mL glass vials and immersed in 1 mL of lysis buffer (5% SDS, 50 mM pH 8.5 Tris-HCl, 0.15 M NaCl, 0.1 mM EDTA, 1 mM $MgCl_2$, and 50 mM DTT). Subsequent steps of cell lysis, protein extraction, and tryptic digestion followed established procedures.[33,34] An aliquot equivalent to 75 μg of peptides was loaded onto a biphasic resin Luna SCX and Aqua C_{18} packed column (Phenomenex, Torrance, CA, USA). Peptide separation was performed with an 11-salt pulse chromatographic separation strategy for a total of 22 h using an Ultimate 3000 HPLC system (Thermo Scientific), and peptide spectral data were collected in a data-dependent mode with an LTQ-XL mass spectrometer (Thermo Scientific), as described.[35]

Computational Analysis. For protein identification, the raw spectra were searched against protein sequences derived from the strain FL2 genome[21] via the MyriMatch version 2.1 algorithm using described parameters with minor modifications.[36] Identification required at least two peptides (one unique and one non-unique) per protein. Common laboratory contaminant protein sequences were concatenated and included in the database. A false discovery rate cutoff for peptide to spectrum identification was maintained at less than 1% and was calculated using reverse database sequences as decoys. For downstream data analysis, spectral counts of identified peptides were processed to obtain normalized spectral counts (nSpc).[37] To calculate the nSpc values, the spectral count obtained for each protein was divided by the length of the protein to account for the effect of protein size. In general, larger proteins tend to contribute more peptides and therefore more spectral counts than smaller proteins. To minimize the effects of run-to-run variation, each length normalized spectral count value was then divided by the sum of all these values for all proteins in the experiment. The obtained numbers were then scaled by multiplying with the average of the totals of the spectral counts in each analysis. To assist visualization, the adjusted nSpc values were transformed to log 2 units.

Analytical Methods. Ethene and chlorinated ethenes were analyzed using an Agilent 7890 gas chromatograph equipped with an Agilent DB-624 capillary column (1.80 μm film thickness, 0.32 mm inner diameter × 60 m length) and a flame ionization detector.[32] The maximum VC dechlorination rates were calculated based on the change of nominal ethene concentrations (μM day^{-1}; assuming one molecule of ethene is produced from one molecule of VC) over a period of linear ethene increase represented by at least three measurements. The overall TCE dechlorination rate (μM Cl^- released day^{-1}) was calculated as the sum of chloride released during each

https://dx.doi.org/10.1021/acs.est.0c07354
Environ. Sci. Technol. 2021, 55, 4831−4841

consecutive dechlorination step based on the measured amounts of *c*DCE, VC and ethene.[7] The first-order growth rate (day^{-1}) was calculated, as described (see the Supporting Information for details).[38]

Data Availability. The resequenced *tceA* genes of strain FL2 and strain 195 have been deposited in GenBank under accession numbers MW561114 and MW561115, respectively. The ABI sequencing data are provided as Supporting Information 1−8. Spectral data from the proteomic analysis were deposited in the MassIVE and ProteomeXchange repositories with identifiers MSV000086254 and PXD021905, respectively.

RESULTS

B_{12} Concentration Affects TCE Dechlorination Rates and Ethene Formation. *Dhc* strain FL2 cultures amended with 1 $\mu g\ L^{-1}$ B_{12} dechlorinated TCE and released inorganic Cl^- at rates of 12.8 ± 5.8 $\mu M\ Cl^-\ day^{-1}$. Dechlorination ceased after a 32-day incubation period, and 11.9 ± 4.8 μmol of *c*DCE and 14.5 ± 6.9 μmol of VC were produced with 21.9 ± 11.1 μmol of remaining TCE without ethene formation (Figure 2A). In cultures that received 10 $\mu g\ L^{-1}$ B_{12}, higher dechlorination rates of 42.3 ± 2.3 $\mu M\ Cl^-$ released day^{-1} were observed, and the initial amount of TCE (57.6 ± 1.0 μmol) was completely dechlorinated to ethene (49.2 ± 2.4 μmol) and VC (8.8 ± 1.2 μmol) after a 39-day incubation period, but complete conversion of VC to ethene was not achieved (Figure 2B). Electron donor limitation cannot explain stalled VC dechlorination because H_2 was provided in excess based on the electron demand for complete TCE reductive dechlorination to ethene. With 25 $\mu g\ L^{-1}$ B_{12}, strain FL2 cultures exhibited dechlorination rates of 43.1 ± 3.1 $\mu M\ Cl^-$ released day^{-1} and completely dechlorinated TCE to ethene (55.8 ± 3.2 μmol) with only small amounts of VC (1.8 ± 0.2 μmol) remaining (Figure 2C). The highest dechlorination rates of 52.4 ± 3.2 $\mu M\ Cl^-$ released day^{-1} were observed in cultures that received 50 $\mu g\ L^{-1}$ B_{12}, and TCE was completely dechlorinated to ethene (Figure 2D). Ethene formation occurred following the consumption of TCE and *c*DCE in cultures with ≥10 $\mu g\ L^{-1}$ B_{12} (Figure 2B−D).

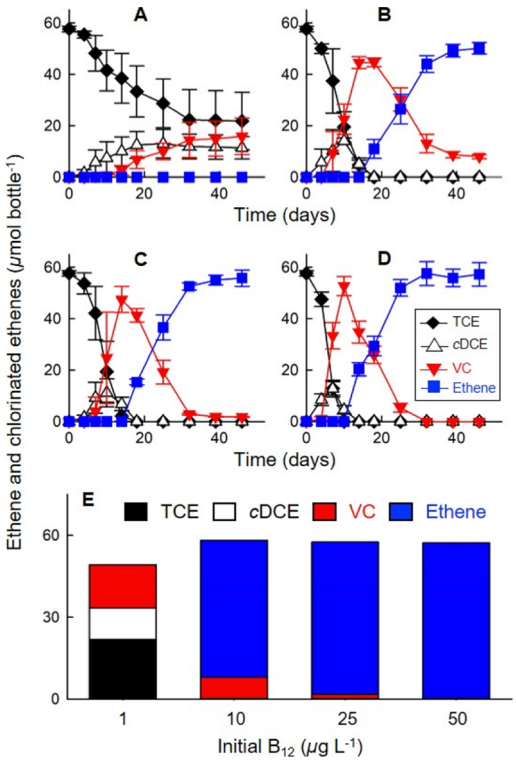

Figure 2. Reductive dechlorination of TCE in *Dhc* strain FL2 cultures amended with different B_{12} concentrations. Panels A to D show cultures that received initial concentrations of 1 (A), 10 (B), 25 (C), and 50 $\mu g\ L^{-1}$ (D) B_{12}. Panel (E) shows the amounts of TCE, *c*DCE, VC, and ethene at the end of the incubation period in culture bottles that received different initial B_{12} concentrations. Error bars represent the standard deviations of triplicate samples and are not shown if they are smaller than the symbols.

The experimental data indicate that the molar fraction of ethene strongly correlated with the starting B_{12} concentration (Figure 2E). Uninoculated control incubations with 50 $\mu g\ L^{-1}$ B_{12} did not show any TCE or VC dechlorination, consistent with previous studies demonstrating that B_{12}-mediated abiotic dechlorination requires orders of magnitude higher B_{12} concentrations (i.e., >10 mg L^{-1}) and the presence of a strong reductant such as titanium(III).[39] Taken together, these results demonstrate that elevated B_{12} concentrations increased TCE dechlorination rates and supported complete reductive dechlorination of TCE to ethene in strain FL2 cultures.

Respiratory VC Dechlorination Depends on the Starting B_{12} Concentration. Motivated by the observation that elevated B_{12} concentrations promoted ethene formation, we investigated the effect of the starting B_{12} concentration on the growth of *tceA*-carrying *Dhc* strains with VC as the sole electron acceptor.

After a 94-day incubation period, no substantial VC dechlorination was observed in strain FL2 cultures that received 1 $\mu g\ L^{-1}$ B_{12}. No more than 16% of the initial 80.9 ± 0.9 μmol of VC was dechlorinated to ethene (Figure 3A), which corresponded to a VC dechlorination rate of 0.99 ± 0.13 $\mu M\ day^{-1}$. Strain FL2 cultures that received 10, 25, and 50 $\mu g\ L^{-1}$ B_{12} completely dechlorinated VC to ethene within 84 days at statistically identical rates of 14.80 ± 1.30 $\mu M\ day^{-1}$ (Figures 3B and S2). qPCR measurements determined that the strain FL2 cell numbers increased about 45-fold following complete dechlorination to ethene, and similar growth yields were determined (Table 1). Similar growth rates of 0.0424 ± 0.0047, 0.0392 ± 0.0040, and 0.0430 ± 0.0045 d^{-1} were calculated in strain FL2 cultures that received 10, 25, and 50 $\mu g\ L^{-1}$ B_{12}, respectively. In contrast, strain FL2 cell numbers in cultures that received 1 $\mu g\ L^{-1}$ B_{12} increased no more than two-fold, and the calculated growth yield of 3.34 ± 0.99 × 10^7 cells per μmol of VC consumed was nearly 1 order of magnitude lower compared to cultures that received 10 $\mu g\ L^{-1}$ or more B_{12}. The growth yield data indicate that the initial amount of B_{12} affected the ability of *Dhc* strain FL2 to utilize VC as a respiratory electron acceptor.

Experiments with *Dhc* strain 195 also demonstrated growth with VC as the electron acceptor. Cultivation of strain 195 with 1 $\mu g\ L^{-1}$ B_{12} resulted in slow and incomplete VC dechlorination with no more than 22.9 ± 5.4 μmol (28.1 ± 6.7%) of the initial amount of VC dechlorinated to ethene over a 140-day incubation period (Figure S2). Maximum VC dechlorination rates of 6.00 ± 2.30 $\mu M\ day^{-1}$ were measured between day 28 and day 52, and VC dechlorination activity gradually decreased and ceased (Figure S2). The qPCR measurements determined *Dhc* strain 195 cell numbers of 8.35 ± 2.6 × 10^6 cells mL^{-1} following cessation of VC

https://dx.doi.org/10.1021/acs.est.0c07354
Environ. Sci. Technol. 2021, 55, 4831−4841

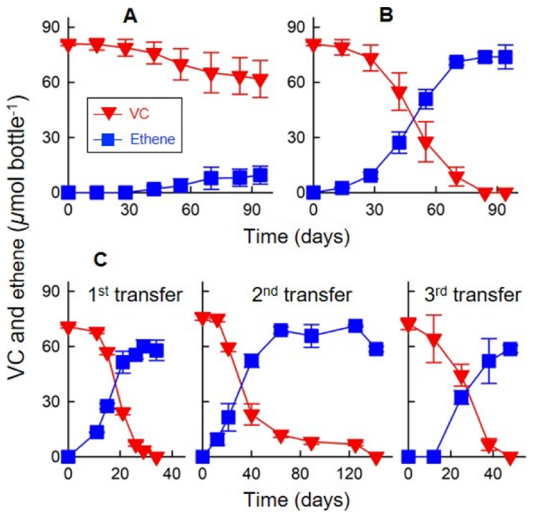

Figure 3. Reductive dechlorination of VC in *Dhc* strain FL2 and strain 195 cultures. Panel A and panel B show VC to ethene reductive dechlorination in strain FL2 cultures that received initial B_{12} concentrations of 1 and 10 $\mu g\ L^{-1}$, respectively. Strain FL2 cultures that received 25 and 50 $\mu g\ L^{-1}$ B_{12} showed nearly identical VC dechlorination and ethene formation patterns as cultures with 10 $\mu g\ L^{-1}$ B_{12}. Panel (C) shows reductive dechlorination of VC to ethene in three consecutive transfers of *Dhc* strain 195 cultures amended with 50 $\mu g\ L^{-1}$ B_{12}. Error bars represent the standard deviations of triplicate samples and are not shown if they are smaller than the symbols.

dechlorination activity, which were not statistically different ($p > 0.1$) from the initial cell numbers of $7.57 \pm 0.98 \times 10^6$ cells mL^{-1}, indicating that *Dhc* growth did not occur in cultures supplied with 1 $\mu g\ L^{-1}$ B_{12} (Table 1). In contrast, strain 195 cultures supplied with 50 $\mu g\ L^{-1}$ B_{12} dechlorinated VC to ethene within 29 days at higher rates of 25.89 ± 1.90 μM VC day^{-1} (Figure 3C, left) and attained growth yields of $1.80 \pm 1.00 \times 10^8$ cells per μmol of VC consumed (Table 1). Strain 195 cultures that received 50 $\mu g\ L^{-1}$ B_{12} could be consecutively transferred with VC as the electron acceptor, and stoichiometric amounts of ethene were produced (Figure 3C). With 50 $\mu g\ L^{-1}$ B_{12}, strain 195 exhibited growth rates of $0.0407 \pm 0.0068\ d^{-1}$, comparable to those observed in strain FL2 cultures that received sufficient (i.e., 10−50 $\mu g\ L^{-1}$) B_{12}.

Taken together, these results demonstrate that the *Dhc* strains harboring the *tceA* gene, but lacking the known VC RDase genes *bvcA*, *vcrA*, or *cerA*, are capable of respiratory VC dechlorination when sufficient B_{12} is supplied. Of note, with 50 $\mu g\ L^{-1}$ B_{12}, the VC dechlorination rates observed in strain 195 cultures (25.9 μM VC day^{-1}; final density of $1.13 \pm 0.63 \times 10^8$ cells mL^{-1}) were about 75% higher than those observed in strain FL2 cultures (14.8 μM VC day^{-1}; final density of $1.25 \pm 0.88 \times 10^8$ cells mL^{-1}). In cultures of *Dhc* strain BAV1, which expresses the VC RDase BvcA during growth with VC, maximum dechlorination rates of 79.01 ± 7.70 μM VC day^{-1} were observed (Figure S2).

Detection of Non-Synonymous Substitutions in *tceA* Genes. Nearly the entire 1665 bp-long strain FL2 *tceA* gene, encoded on the positive-sense strand, was assembled (sequence coverage of 97.72% encompassing positions 18−1644). Upon alignment with the previously deposited strain FL2 *tceA* gene sequence (GenBank accession number AY165309),[20] a single-nucleotide substitution (G to A) was identified at position 412 on the positive-sense strand (Figure 4A). Consequently, the codon GAA (glutamic acid) changed to an AAA codon (lysine). The presence of this non-synonymous substitution was confirmed at the corresponding position on the negative-sense strand (Figure 4B) obtained

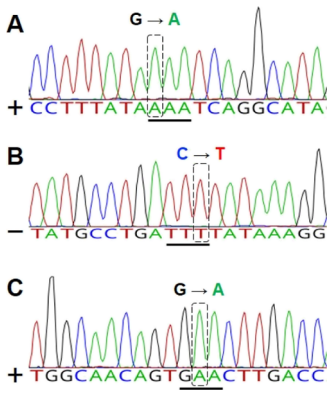

Figure 4. Sanger sequencing identified non-synonymous substitutions in *tceA* genes. The top panel (A) illustrates a G-to-A nucleotide substitution at the 412 bp position in the positive-sense strand (coding sequence) of strain FL2's *tceA* gene. (B) This substitution was confirmed at the corresponding position in the negative-sense strand (non-coding sequence) of strain FL2's *tceA* gene. The bottom panel (C) shows a G-to-A nucleotide substitution identified in the positive-sense strand (non-coding sequence) of strain 195's *tceA* gene, corresponding to a C-to-T substitution at the 1520 bp position in the negative-sense strand (coding sequence).

Table 1. Growth of *Dhc* Strain FL2 and Strain 195 with VC as the Electron Acceptor in Defined Medium with Different Initial B_{12} Concentrations

			Dhc cell numbers (mL^{-1})[b]			
Dhc	B_{12} ($\mu g\ L^{-1}$)	ethene produced (μmol per bottle)	initial	final	fold increase[c]	growth yield[d]
strain FL2	1	9.50 ± 4.91	$2.83 \pm 0.24 \times 10^6$	$5.69 \pm 1.09 \times 10^6$	2.0	$3.34 \pm 0.99 \times 10^7$
	10	73.78 ± 6.44[a]	$2.83 \pm 0.24 \times 10^6$	$1.28 \pm 0.13 \times 10^8$	45.2	$1.71 \pm 0.26 \times 10^8$
	25	72.25 ± 4.33[a]	$2.83 \pm 0.24 \times 10^6$	$1.26 \pm 0.23 \times 10^8$	44.5	$1.71 \pm 0.42 \times 10^8$
	50	73.97 ± 0.57[a]	$2.83 \pm 0.24 \times 10^6$	$1.25 \pm 0.88 \times 10^8$	44.2	$1.64 \pm 0.11 \times 10^8$
strain 195	1	22.36 ± 4.01	$7.57 \pm 0.98 \times 10^6$	$8.35 \pm 2.60 \times 10^6$	1.1	[f]
	50	58.59 ± 1.98[a]	$4.66 \pm 0.40 \times 10^{6}$[e]	$1.13 \pm 0.63 \times 10^{8}$[e]	24.2	$1.80 \pm 1.00 \times 10^8$

[a]The initial amount of VC was completely dechlorinated to ethene at the end of incubation. [b]*Dhc* cell numbers were determined with qPCR targeting the *tceA* gene. Average and standard deviation of *tceA* gene copy numbers were calculated from triplicate cultures. [c]Fold increase in cell densities is reported as averages of triplicate cultures. [d]Growth yields were calculated as increases of cells per μmol of ethene produced. [e]Cell numbers were measured in the third transfer of strain 195 VC-dechlorinating cultures. [f]No growth occurred.

https://dx.doi.org/10.1021/acs.est.0c07354
Environ. Sci. Technol. 2021, 55, 4831−4841

using the TceA1336R primer and was also apparent in the *tceA* gene (locus tag number DhcFL2_01280) on the recently sequenced strain FL2 genome.[21]

Similarly, the *tceA* gene of strain 195 encoded on the negative-sense strand was assembled with a sequence coverage of 97.32% encompassing positions 16−1615. By comparing with the *tceA* gene (locus tag DET_RS00495) on the strain 195 genome reported 15 years ago,[40] a single-nucleotide substitution (G to A) was identified on the positive-sense strand obtained using the 2490R primer (Figure 4C). This substitution reflected a C-to-T nucleotide change at the 1520 bp position in the negative-sense strand (i.e., the coding sequence) and caused a non-synonymous substitution of a TCC codon (serine) to the TTC codon (phenylalanine). The Sanger sequencing efforts demonstrated that mutations changed the *tceA* gene of strain FL2 and strain 195 during repeat transfers over a 15-year time span.

Proteomic Profiling Implicates TceA in Respiratory VC Reductive Dechlorination. The presence of multiple, non-identical putative RDase genes is a shared feature of sequenced *Dhc* genomes.[41] For example, 24 and 18 non-identical RDase genes, including *tceA*, are present on the strain FL2 and strain 195 genomes, respectively (Table S2).[21,40] To determine if TceA, or possibly an uncharacterized RDase, enabled respiratory VC dechlorination, global proteomic analysis was performed using VC-grown strain FL2 cells.

A total of 516 *Dhc* proteins (Table S4) were detected, with chaperon-like proteins and some hypothetical proteins being the most abundantly expressed. 31 and 47 RDase peptides, including YFGASSVGAIK, YEGSRPYLSMR, and WEGT-PEENLLIMR that can be uniquely assigned to TceA, were detected across two technical LC−MS/MS replicate runs. In either run, TceA was the only RDase amongst the top 20 most abundantly expressed proteins based on the relative spectral counts of TceA-unique peptides (Table S5). In addition to TceA, the proteomic analysis detected a total of 37 and 62 unique peptides with assignment to six putative RDases, which did not cluster phylogenetically with TceA or characterized VC RDases (Figure 1), and were estimated to be present in 2.2- to 100-fold lower relative abundances than TceA based on their average nSpc values (Table S6). Three of these detected putative RDases (gene locus tag numbers DhcFL2_07110, DhcFL2_07240, and DhcFL2_06670) grouped with MbrA,[42] an RDase demonstrated to dechlorinate TCE to a mixture of DCE isomers.[43]

The only other corrinoid-dependent enzyme expressed during growth with VC was class II ribonucleotide reductase (RNR). The strain FL2 genome harbors four non-identical copies of the class II RNR gene (locus tag numbers DhcFL2_01175, DhcFL2_01305, DhcFL2_01505, and DhcFL2_02820), of which only the RNR encoded by DhcFL2_02820 was detected in low abundance (Table S4). These results demonstrate that TceA was the most abundant corrinoid-dependent enzyme expressed in strain FL2 and support the involvement of TceA in respiratory VC dechlorination.

B_{12} Depletion in Cultures Utilizing VC as Electron Acceptor. In *Dhc* strain FL2 and strain 195 cultures with VC as the electron acceptor and 1 $\mu g\ L^{-1}$ B_{12}, very limited growth and dechlorination activity were observed, and B_{12} was depleted below the method detection limit of 0.05 $\mu g\ L^{-1}$. Substantial B_{12} uptake also occurred in VC-dechlorinating strain FL2 and strain 195 cultures that received 10 $\mu g\ L^{-1}$ or higher concentrations of B_{12}. In strain FL2 cultures, the initial amount of 10 $\mu g\ L^{-1}$ B_{12} (measured initial amount was 9.73 ± 0.54 $\mu g\ L^{-1}$) decreased to 1.26 ± 0.23 $\mu g\ L^{-1}$, accounting for an 84−88% loss of B_{12} (Figure 5). *Dhc* strain 195 cultures used

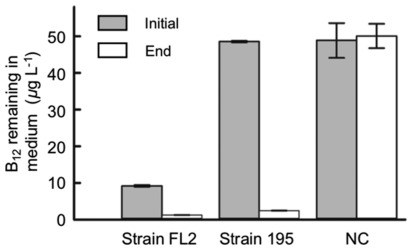

Figure 5. B_{12} uptake in VC-dechlorinating *Dhc* strain FL2 and strain 195 cultures. Chemical stability of B_{12} was demonstrated in NC bottles without inoculum. Error bars represent the standard deviations of triplicate samples.

nearly 95% of the initial amount of 50 $\mu g\ L^{-1}$ B_{12} (measured initial amount was 48.55 ± 0.01 $\mu g\ L^{-1}$) following the complete consumption of VC (Figure 5). In contrast to the VC-dechlorinating cultures, B_{12} concentrations remained statistically indifferent (i.e., initial vs final concentrations of 48.85 ± 4.74 and 50.07 ± 3.34 $\mu g\ L^{-1}$) in NC incubations (Figure 5).

DISCUSSION

At sites impacted with chlorinated solvents (e.g., PCE and TCE), complete reductive dechlorination to non-toxic ethene is required to achieve detoxification and meet groundwater remedial goals and regulations. Therefore, groundwater monitoring regimes that measure biomarkers of VC-respiring *Dhc* has prognostic and diagnostic value for site management decision-making and assessing a site's trajectory toward site closure.[24,28] Laboratory studies have characterized *Dhc* strains carrying *tceA* as TCE and DCE dechlorinators that lack the ability to utilize VC as a respiratory electron acceptor.[20,23] Although the *tceA* gene is not recognized as a biomarker for VC detoxification, *tceA* is often one of the most abundant RDase genes in chlorinated solvent plumes.[24,44] Our new findings demonstrate that TceA can function as a VC RDase and *tceA*-carrying *Dhc* strains grow with VC as a respiratory electron acceptor as long as the demand for B_{12} is met.

B_{12} Availability Can Affect *Dhc* Phenotype. The complete form of corrinoids are known as cobamides, which consist of a cobalt-containing tetrapyrrole ring, an upper ligand, and a lower base.[45] Cobalamin, the biologically active form of vitamin B_{12}, carries DMB as the lower base and is a preferred prosthetic group for corrinoid-auxotrophic *Dhc*.[32] The B_{12} availability affects *Dhc* dechlorination rates and dechlorination endpoints.[7,46,47] In strain 195 cultures, an increase from 1 to 25 $\mu g\ L^{-1}$ B_{12} doubled the TCE dechlorination rates and growth yields and also resulted in higher final ethene-to-VC ratios; however, growth with VC as the electron acceptor was not observed.[46] Similarly, efforts to grow *Dhc* strain FL2 with VC as the electron acceptor were not successful.[20] The results presented here demonstrate that B_{12} availability determines the ability of *Dhc* strain FL2 and strain 195 to perform respiratory VC dechlorination, a new physiological trait for *tceA*-carrying *Dhc* strains. The conclusion that TceA is a respiratory VC RDase is supported by multiple lines of evidence including the dechlorination of VC to

https://dx.doi.org/10.1021/acs.est.0c07354
Environ. Sci. Technol. 2021, 55, 4831−4841

stoichiometric amounts of ethene, growth in consecutive transfer cultures in defined mineral salt medium with VC as the electron acceptor, growth yields with VC on par with values reported for *Dhc* strains carrying *bvcA* and *vcrA*,[7,12] and the expression of TceA during growth with VC.

The reasons why earlier studies could not demonstrate growth of *Dhc* strain 195 and strain FL2 with VC are unclear. While the failure to grow strain FL2 cultures that received one or multiple doses of 1 μg L^{-1} B_{12} with VC as the electron acceptor can be explained by inadequate B_{12} supply,[12,20] prior attempts have used up to 200 μg L^{-1} B_{12} to grow *Dhc* strain 195.[46] An intriguing explanation is that genetic changes (i.e., mutations) may have occurred during long-term (i.e., >15 years) laboratory cultivation and altered the functionality of *tceA*. Our laboratory routinely transfers actively dechlorinating *Dhc* cultures monthly to fresh medium. TCE-grown *Dhc* strain FL2 cultures generally attain cell densities of about $1.2-1.4 \times 10^8$ cells mL^{-1}, and transfer cultures are initiated with an inoculum size of 1−3% (v/v). We calculated that about 900−1200 generations have occurred between the prior, unsuccessful efforts to grow *Dhc* strain FL2 with VC as the electron acceptor[20]. This study detected single-nucleotide nonsynonymous mutations in both the *tceA* gene sequences of strain FL2 and strain 195. Since the structure of TceA has not been resolved, the consequences of specific amino acid changes on TceA function are unknown. Minor sequence changes can affect RDase function, as has been documented for the *cfrA* and *dcrA* RDase genes, which share 97.8% sequence identity but the respective enzymes have distinct dechlorination activities (i.e., CfrA dechlorinates chloroform and 1,1,1-trichloroethane, whereas DcrA dechlorinates 1,1-dichloroethane).[48]

Despite progress, the regulation and biochemistry of organohalide respiration remain poorly understood compared to other microbial respiratory processes.[3,4,49] Hence, mutations in genes encoding other components of the organohalide respiratory chain could also affect chemiosmotic coupling and TceA-catalyzed reductive dechlorination of VC. Genome resequencing and proteogenomic studies are warranted to further explore whether the observed phenotypic changes have a genetic underpinning in *Dhc* strain FL2 and strain 195. Such efforts can shed light on potential mechanisms that alter (i.e., expand) the range of chlorinated electron acceptors an RDase dechlorinates or an existing respiratory chain can utilize for energy conservation. From a practical point of view, a refined understanding of the mechanisms and processes that can lead to new phenotypes with expanded dechlorination capabilities is of great interest for predicting the fate and longevity of environmental pollutants.

High B_{12} Demand Suggests a Corrinoid Sink in *Dhc* Cells. To date, all *Dehalococcoidia* share the obligate organohalide-respiring lifestyle that hinges on cobamide-dependent RDases.[12] As corrinoid auxotrophs, *Dhc* and *Dehalogenimonas* spp. have to scavenge adequate amounts of complete cobamides or precursor molecules to enable the maturation of RDases for energy conservation. For laboratory cultivation of *Dehalococcoidia* isolates, B_{12} has been commonly supplied in the range of 25−50 μg L^{-1}.[32,46,50−53] During growth with TCE, targeted proteomic analysis quantified averages of 7.6×10^3 and 1.8×10^3 TceA proteins per *Dhc* cell in consortium KB-1 and consortium SDC-9, respectively.[54,55] Assuming each TceA protein contains one cobamide molecule (i.e., a 1:1 ratio),[56,57] the theoretical B_{12} demand to reach the observed cell densities (Table 1) would be 0.5−2.4 and 0.3−2.7 μg L^{-1} for *Dhc* strain FL2 and strain 195, respectively (eq 1).

$$\begin{aligned} &B_{12}\ \text{demand}\ (\mu\text{g L}^{-1}) \\ &= (\text{cell density [cells mL}^{-1}])(\text{TceA proteins [cell}^{-1}]) \\ &\times \left(\frac{10^3\ \text{mL}}{1\ \text{L}}\right)\left(\frac{1\ \text{mol}}{6.023 \times 10^{23}}\right)\left(\frac{1355.4\ \text{g}}{\text{mol}}\right)\left(\frac{10^6\ \mu\text{g}}{1\ \text{g}}\right) \end{aligned} \quad (1)$$

In contrast to this calculated B_{12} demand, the actual B_{12} uptake from the growth medium was far greater. For instance, strain 195 cultures with an initial B_{12} concentration of 50 μg L^{-1} (measured amount was 48.55 ± 0.01 μg L^{-1}) used 46.06 ± 0.01 μg L^{-1} (i.e., 95%) of the initial amount of B_{12} provided. The reasons why the B_{12} uptake exceeds the direct needs for respiratory VC dechlorination in *Dhc* strain 195 and strain FL2 are unclear. *Dhc* strains possess the bacterial corrinoid uptake system and are highly efficient corrinoid scavengers.[6,58] The regulation of the corrinoid uptake machinery in *Dhc* has not been explored but considering that energy conservation in *Dhc* strictly depends on exogenous corrinoids, constitutive expression is conceivable. An interesting question to explore is the ability of *Dhc* to store corrinoid intracellularly to maintain organohalide-respiring activity during corrinoid famine. The obvious gap between theoretical B_{12} demand and actual B_{12} uptake cannot be explained with the current knowledge of *Dhc* biology. Whether this higher-than-expected B_{12} demand is specific for *Dhc* strains expressing TceA or a general phenomenon associated with *Dhc* is unclear.

Ecological Inferences. A recent bioinformatics-based survey predicated that only 37% of sequenced bacterial genomes are capable of *de novo* corrinoid biosynthesis.[59] Corrinoids are generally depleted in environmental systems, and concentrations of 14 ng L^{-1} (10 pM) have been reported in freshwater ecosystems.[60] Total corrinoids were also quantified in seawater along the northeast pacific coast and concentrations ranged from undetectable to 41 ng L^{-1}.[61] The low corrinoid concentrations (i.e., ng L^{-1} level) in environmental systems imply fierce competition among corrinoid auxotrophs, putting organisms such as *Dhc* with a high B_{12} demand (i.e., μg L^{-1} level) in a precarious position.

Although data for corrinoid types and concentrations in groundwater aquifers are not available, the indigenous corrinoid pool is unlikely to meet *Dhc* strains' μg L^{-1} level B_{12} demand to achieve maximum growth yields and dechlorination activity. Groundwater monitoring data indicated that meaningful *in situ* dechlorination activity and ethene formation can be achieved when *Dhc* cell titers exceed 10^6 L^{-1}.[27,28] Assuming 1.8×10^3 to 7.6×10^3 RDase (e.g., TceA) proteins per *Dhc* cell[54,55] and a cobamide-to-RDase molar ratio of 1:1, 8.1 to 34 pg L^{-1} of B_{12} should theoretically meet the corrinoid demand of 10^6 *Dhc* cells L^{-1} and allow *in situ* bioremediation to take place. Therefore, it is conceivable that *in situ* aquifer conditions exist that sustain *Dhc* reductive dechlorination activity even at meager (i.e., ng L^{-1}) corrinoid pool sizes.

Dhc strains possess the high-affinity BtuFCD-type corrinoid uptake system to scavenge low concentrations (ng L^{-1}) of cobalamin or B_{12} derivatives.[6,7] In addition, *Dhc* genomes encode both the archaeal CbiZ-type and the bacterial CobU-type corrinoid salvage systems, enabling the assembly of

https://dx.doi.org/10.1021/acs.est.0c07354
Environ. Sci. Technol. 2021, 55, 4831−4841

incomplete cobamides (e.g., cobinamide) or remodel unfavorable cobamides into cobalamin in the presence of DMB.[32,58] The binding affinity (15 nM) and dissociation constant K_d ($\sim 10^{-4}$ nM) of B_{12} to the periplasmic cobalamin-binding protein BtuF has been characterized in *Escherichia coli*.[62,63] Either the BtuF of *Dhc* binds corrinoid more efficiently or a sufficiently high corrinoid flux exists *in situ* allowing *Dhc* to scavenge enough corrinoid.

Unfortunately, knowledge about corrinoid fluxes in environmental systems is largely lacking; however, a number of studies demonstrated enhanced robustness of *Dhc* dechlorination activity in mixed cultures compared to axenic growth.[46,64−66] The improved reductive dechlorination performance was attributed to interspecies hydrogen transfer and the supply of growth factors, in particular cobamides. Co-cultivation studies with corrinoid prototrophs (e.g., methanogens, fermenters, other OHRB) demonstrated the formation of aggregates.[66−69] The rate at which cobamides are made available to *Dhc* in such microbial assemblages is unclear, but it is conceivable that interactions within such aggregates support *Dhc*'s nutritional requirements. Future studies should attempt measuring corrinoid fluxes from a producer to a consumer (i.e., *Dhc*) and unravel if the nature of these interactions is mutualistic (i.e., bidirectional) or commensal (i.e., unidirectional). Considering the commonality of corrinoid-dependent enzyme systems and the prevalence of corrinoid auxotrophy in the microbial world,[8,59] elucidating the strategies of organisms that lack the ability for *de novo* corrinoid biosynthesis should be a priority goal in microbial ecology research.

Implications for Bioremediation. At sites contaminated with chlorinated ethenes where bioremediation has been implemented, qPCR-based monitoring regimes generate information about the abundance of *Dhc* and the RDase genes *tceA*, *vcrA*, and *bvcA*. Only the latter two genes are recognized as biomarkers for VC detoxification but *tceA* is not. Consequently, a sample with high abundance of *tceA* but lacking *vcrA* and *bvcA* genes would lead to the conclusion that VC formation is likely but detoxification to ethene is not.[24] The findings reported here demonstrate that TceA supports respiratory VC reductive dechlorination and that *Dhc* strains harboring *tceA* can grow with VC as the electron acceptor. Therefore, *tceA* serves as an indicator for ethene formation and monitoring data showing high *tceA* but low *vcrA* and *bvcA* abundances should not be interpreted as a lack of VC detoxification potential. In support of this recommendation, a recent survey of 859 groundwater samples representing 62 sites undergoing monitored natural attenuation or enhanced remediation found a positive correlation between the *tceA* gene abundances and ethene formation.[24]

Scientific reports about the corrinoid demand for *Dhc* has triggered bioremediation vendors to include B_{12} in electron donor formulations to promote *in situ* *Dhc* reductive dechlorination activity. Although laboratory experiments have demonstrated the benefits of elevated B_{12} for efficient dechlorination to non-toxic ethene, scientific data supporting the injection of B_{12} into groundwater aquifer are lacking. Competition and rapid uptake of B_{12} by fast-growing corrinoid auxotrophs and prototrophs will most likely limit the success of such a strategy.

■ ASSOCIATED CONTENT

Supporting Information

The Supporting Information is available free of charge at https://pubs.acs.org/doi/10.1021/acs.est.0c07354.

RDases with assigned functions and their host OHRB; predicted products of the putative RDase genes annotated in *Dhc* strain 195 and strain FL2 genomes; nucleotide sequences of the primers and probe used in this study for *tceA*-targeted PCR, qPCR, and Sanger sequencing; protein expression in a *Dhc* strain FL2 culture grown with VC; top 20 most abundant proteins expressed in *Dhc* strain FL2 cultures grown with VC as the electron acceptor; TceA and putative RDases expressed in *Dhc* strain FL2 cultures grown with VC as the electron acceptor; sensitive detection and quantification of B_{12} using a mass spectrometry-based approach; and reductive dechlorination of VC in axenic *Dhc* cultures with different B_{12} concentrations (PDF)

Protein expression in a *Dhc* strain FL2 culture grown with VC (XLSX)

Strain FL2 TceA1270F (PDF)

Strain FL2 797F (PDF)

Strain 195 797F (PDF)

Strain 195 2490R (PDF)

Strain FL2 2490R (PDF)

Strain FL2 TceA1336R (PDF)

Strain 195 TceA1270F (PDF)

Strain 195 TceA1336R (PDF)

■ AUTHOR INFORMATION

Corresponding Authors

Jun Yan − *Key Laboratory of Pollution Control and Environmental Engineering, Institute of Applied Ecology, Chinese Academy of Sciences, Shenyang, Liaoning 110016, China; Department of Microbiology, University of Tennessee, Knoxville, Tennessee 37996, United States*; Phone: +86-2483970426; Email: junyan@iae.ac.cn

Frank E. Löffler − *Department of Microbiology, Center for Environmental Biotechnology, Department of Civil and Environmental Engineering, and Department of Biosystems Engineering & Soil Science, University of Tennessee, Knoxville, Tennessee 37996, United States; Biosciences Division and Joint Institute for Biological Sciences (JIBS), Oak Ridge National Laboratory, Oak Ridge, Tennessee 37831, United States*; orcid.org/0000-0002-9797-4279; Phone: +1-8659744933; Email: frank.loeffler@utk.edu

Authors

Jingjing Wang − *Key Laboratory of Pollution Control and Environmental Engineering, Institute of Applied Ecology, Chinese Academy of Sciences, Shenyang, Liaoning 110016, China; University of Chinese Academy of Sciences, Beijing 100049, China*

Manuel I. Villalobos Solis − *Biosciences Division, Oak Ridge National Laboratory, Oak Ridge, Tennessee 37831, United States*

Huijuan Jin − *Key Laboratory of Pollution Control and Environmental Engineering, Institute of Applied Ecology, Chinese Academy of Sciences, Shenyang, Liaoning 110016, China; University of Chinese Academy of Sciences, Beijing 100049, China*

https://dx.doi.org/10.1021/acs.est.0c07354
Environ. Sci. Technol. 2021, 55, 4831−4841

Karuna Chourey − *Biosciences Division, Oak Ridge National Laboratory, Oak Ridge, Tennessee 37831, United States*
Xiuying Li − *Key Laboratory of Pollution Control and Environmental Engineering, Institute of Applied Ecology, Chinese Academy of Sciences, Shenyang, Liaoning 110016, China*
Yi Yang − *Key Laboratory of Pollution Control and Environmental Engineering, Institute of Applied Ecology, Chinese Academy of Sciences, Shenyang, Liaoning 110016, China*; orcid.org/0000-0002-3519-5472
Yongchao Yin − *Department of Microbiology, University of Tennessee, Knoxville, Tennessee 37996, United States*
Robert L. Hettich − *Biosciences Division, Oak Ridge National Laboratory, Oak Ridge, Tennessee 37831, United States*; orcid.org/0000-0001-7708-786X

Complete contact information is available at: https://pubs.acs.org/10.1021/acs.est.0c07354

Notes

The authors declare no competing financial interest.

■ ACKNOWLEDGMENTS

This work was supported by the Strategic Environmental Research and Development Program (SERDP project ER-2312), with additional support provided by the National Institute of Environmental Health Sciences (award R01ES024294), and by the National Natural Science Foundation of China (grant numbers 41673126, 41977295, and 41907287).

■ REFERENCES

(1) Leys, D.; Adrian, L.; Smidt, H. Organohalide respiration: microbes breathing chlorinated molecules. *Philos. Trans. R. Soc., B* **2013**, *368*, 20120316.
(2) Hug, L. A.; Maphosa, F.; Leys, D.; Löffler, F. E.; Smidt, H.; Edwards, E. A.; Adrian, L. Overview of organohalide-respiring bacteria and a proposal for a classification system for reductive dehalogenases. *Philos. Trans. R. Soc., B* **2013**, *368*, 20120322.
(3) Schubert, T.; Adrian, L.; Sawers, R. G.; Diekert, G. Organohalide respiratory chains: composition, topology and key enzymes. *FEMS Microbiol. Ecol.* **2018**, *94*, fiy035 DOI: 10.1093/femsec/fiy035.
(4) Fincker, M.; Spormann, A. M. Biochemistry of catabolic reductive dehalogenation. *Annu. Rev. Biochem.* **2017**, *86*, 357−386.
(5) Yan, J.; Bi, M.; Bourdon, A. K.; Farmer, A. T.; Wang, P.-H.; Molenda, O.; Quaile, A. T.; Jiang, N.; Yang, Y.; Yin, Y.; Şimşir, B.; Campagna, S. R.; Edwards, E. A.; Löffler, F. E. Purinyl-cobamide is a native prosthetic group of reductive dehalogenases. *Nat. Chem. Biol.* **2018**, *14*, 8−14.
(6) Yan, J.; Ritalahti, K. M.; Wagner, D. D.; Löffler, F. E. Unexpected specificity of interspecies cobamide transfer from *Geobacter* spp. to organohalide-respiring *Dehalococcoides mccartyi* strains. *Appl. Environ. Microbiol.* **2012**, *78*, 6630−6636.
(7) Yan, J.; Im, J.; Yang, Y.; Löffler, F. E. Guided cobalamin biosynthesis supports *Dehalococcoides mccartyi* reductive dechlorination activity. *Philos. Trans. R. Soc., B* **2013**, *368*, 20120320.
(8) Sokolovskaya, O. M.; Shelton, A. N.; Taga, M. E. Sharing vitamins: cobamides unveil microbial interactions. *Science* **2020**, *369*, eaba0165.
(9) Lovley, D. R. Cleaning up with genomics: applying molecular biology to bioremediation. *Nat. Rev. Microbiol.* **2003**, *1*, 35−44.
(10) Löffler, F. E.; Edwards, E. A. Harnessing microbial activities for environmental cleanup. *Curr. Opin. Biotechnol.* **2006**, *17*, 274−284.
(11) Jugder, B.-E.; Ertan, H.; Lee, M.; Manefield, M.; Marquis, C. P. Reductive dehalogenases come of age in biological destruction of organohalides. *Trends Biotechnol.* **2015**, *33*, 595−610.
(12) Löffler, F. E.; Yan, J.; Ritalahti, K. M.; Adrian, L.; Edwards, E. A.; Konstantinidis, K. T.; Müller, J. A.; Fullerton, H.; Zinder, S. H.; Spormann, A. M. *Dehalococcoides mccartyi* gen. nov., sp. nov., obligately organohalide-respiring anaerobic bacteria relevant to halogen cycling and bioremediation, belong to a novel bacterial class, *Dehalococcoidia* classis nov., order *Dehalococcoidales* ord. nov. and family *Dehalococcoidaceae* fam. nov., within the phylum *Chloroflexi*. *Int. J. Syst. Evol. Microbiol.* **2013**, *63*, 625−635.
(13) Yang, Y.; Higgins, S. A.; Yan, J.; Şimşir, B.; Chourey, K.; Iyer, R.; Hettich, R. L.; Baldwin, B.; Ogles, D. M.; Löffler, F. E. Grape pomace compost harbors organohalide-respiring *Dehalogenimonas* species with novel reductive dehalogenase genes. *ISME J.* **2017**, *11*, 2767−2780.
(14) Bradley, P. M.; Chapelle, F. H. Accumulation of dechlorination daughter products: a valid metric of chloroethene biodegradation. *Remediation* **2007**, *17*, 7−22.
(15) Agency for Toxic Substances and Disease Registry. *Public Health Statement for Vinyl Chloride*; US Department of Health and Human Services, 2006. https://www.atsdr.cdc.gov/ToxProfiles/tp20-c1-b.pdf.
(16) He, J.; Ritalahti, K. M.; Yang, K.-L.; Koenigsberg, S. S.; Löffler, F. E. Detoxification of vinyl chloride to ethene coupled to growth of an anaerobic bacterium. *Nature* **2003**, *424*, 62−65.
(17) Krajmalnik-Brown, R.; Hölscher, T.; Thomson, I. N.; Saunders, F. M.; Ritalahti, K. M.; Löffler, F. E. Genetic identification of a putative vinyl chloride reductase in *Dehalococcoides* sp. strain BAV1. *Appl. Environ. Microbiol.* **2004**, *70*, 6347−6351.
(18) Müller, J. A.; von Abendroth, G.; Meshulam-Simon, G.; McCarty, P. L.; Spormann, A. M. Molecular identification of the catabolic vinyl chloride reductase from *Dehalococcoides* sp. strain VS and its environmental distribution. *Appl. Environ. Microbiol.* **2004**, *70*, 4880−4888.
(19) Magnuson, J. K.; Romine, M. F.; Burris, D. R.; Kingsley, M. T. Trichloroethene reductive dehalogenase from *Dehalococcoides ethenogenes*: Sequence of *tceA* and substrate range characterization. *Appl. Environ. Microbiol.* **2000**, *66*, 5141−5147.
(20) He, J.; Sung, Y.; Krajmalnik-Brown, R.; Ritalahti, K. M.; Löffler, F. E. Isolation and characterization of *Dehalococcoides* sp. strain FL2, a trichloroethene (TCE)- and 1,2-dichloroethene-respiring anaerobe. *Environ. Microbiol.* **2005**, *7*, 1442−1450.
(21) Yan, J.; Yang, Y.; Li, X.; Löffler, F. E. Complete genome sequence of *Dehalococcoides mccartyi* strain FL2, a trichloroethene-respiring anaerobe isolated from pristine freshwater sediment. *Microbiol. Resour. Announce.* **2019**, *8*, e00558−19.
(22) Molenda, O.; Quaile, A. T.; Edwards, E. A. *Dehalogenimonas* sp. strain WBC-2 genome and identification of its *trans*-dichloroethene reductive dehalogenase, TdrA. *Appl. Environ. Microbiol.* **2016**, *82*, 40−50.
(23) Maymó-Gatell, X.; Anguish, T.; Zinder, S. H. Reductive dechlorination of chlorinated ethenes and 1, 2-dichloroethane by "*Dehalococcoides ethenogenes*" 195. *Appl. Environ. Microbiol.* **1999**, *65*, 3108−3113.
(24) Clark, K.; Taggart, D. M.; Baldwin, B. R.; Ritalahti, K. M.; Murdoch, R. W.; Hatt, J. K.; Löffler, F. E. Normalized quantitative PCR measurements as predictors for ethene formation at sites impacted with chlorinated ethenes. *Environ. Sci. Technol.* **2018**, *52*, 13410−13420.
(25) Şimşir, B.; Yan, J.; Im, J.; Graves, D.; Löffler, F. E. Natural attenuation in streambed sediment receiving chlorinated solvents from underlying fracture networks. *Environ. Sci. Technol.* **2017**, *51*, 4821−4830.
(26) Lendvay, J. M.; Löffler, F. E.; Dollhopf, M.; Aiello, M. R.; Daniels, G.; Fathepure, B. Z.; Gebhard, M.; Heine, R.; Helton, R.; Shi, J.; Krajmalnik-Brown, R.; Major, C. L.; Barcelona, M. J.; Petrovskis, E.; Hickey, R.; Tiedje, J. M.; Adriaens, P. Bioreactive barriers: A comparison of bioaugmentation and biostimulation for chlorinated solvent remediation. *Environ. Sci. Technol.* **2003**, *37*, 1422−1431.

(27) Lu, X.; Wilson, J. T.; Kampbell, D. H. Relationship between *Dehalococcoides* DNA in ground water and rates of reductive dechlorination at field scale. *Water Res.* **2006**, *40*, 3131−3140.
(28) Ritalahti, K. M.; Hatt, J. K.; Lugmayr, V.; Henn, K.; Petrovskis, E. A.; Ogles, D. M.; Davis, G. A.; Yeager, C. M.; Lebrón, C. A.; Löffler, F. E. Comparing on-site to off-site biomass collection for *Dehalococcoides* biomarker gene quantification to predict in situ chlorinated ethene detoxification potential. *Environ. Sci. Technol.* **2010**, *44*, 5127−5133.
(29) Kearse, M.; Moir, R.; Wilson, A.; Stones-Havas, S.; Cheung, M.; Sturrock, S.; Buxton, S.; Cooper, A.; Markowitz, S.; Duran, C.; Thierer, T.; Ashton, B.; Meintjes, P.; Drummond, A. Geneious Basic: An integrated and extendable desktop software platform for the organization and analysis of sequence data. *Bioinformatics* **2012**, *28*, 1647−1649.
(30) Le, S. Q.; Gascuel, O. An improved general amino acid replacement matrix. *Mol. Biol. Evol.* **2008**, *25*, 1307−1320.
(31) Ritalahti, K. M.; Amos, B. K.; Sung, Y.; Wu, Q.; Koenigsberg, S. S.; Löffler, F. E. Quantitative PCR targeting 16S rRNA and reductive dehalogenase genes simultaneously monitors multiple *Dehalococcoides* strains. *Appl. Environ. Microbiol.* **2006**, *72*, 2765−2774.
(32) Yan, J.; Şimşir, B.; Farmer, A. T.; Bi, M.; Yang, Y.; Campagna, S. R.; Löffler, F. E. The corrinoid cofactor of reductive dehalogenases affects dechlorination rates and extents in organohalide-respiring *Dehalococcoides mccartyi*. *ISME J.* **2016**, *10*, 1092−1101.
(33) Chourey, K.; Jansson, J.; VerBerkmoes, N.; Shah, M.; Chavarria, K. L.; Tom, L. M.; Brodie, E. L.; Hettich, R. L. Direct cellular lysis/protein extraction protocol for soil metaproteomics. *J. Proteome Res.* **2010**, *9*, 6615−6622.
(34) Chourey, K.; Nissen, S.; Vishnivetskaya, T.; Shah, M.; Pfiffner, S.; Hettich, R. L.; Löffler, F. E. Environmental proteomics reveals early microbial community responses to biostimulation at a uranium- and nitrate-contaminated site. *Proteomics* **2013**, *13*, 2921−2930.
(35) Sharma, R.; Dill, B. D.; Chourey, K.; Shah, M.; VerBerkmoes, N. C.; Hettich, R. L. Coupling a detergent lysis/cleanup methodology with intact protein fractionation for enhanced proteome characterization. *J. Proteome Res.* **2012**, *11*, 6008−6018.
(36) Xiong, W.; Giannone, R. J.; Morowitz, M. J.; Banfield, J. F.; Hettich, R. L. Development of an enhanced metaproteomic approach for deepening the microbiome characterization of the human infant gut. *J. Proteome Res.* **2015**, *14*, 133−141.
(37) Paoletti, A. C.; Parmely, T. J.; Tomomori-Sato, C.; Sato, S.; Zhu, D.; Conaway, R. C.; Conaway, J. W.; Florens, L.; Washburn, M. P. Quantitative proteomic analysis of distinct mammalian Mediator complexes using normalized spectral abundance factors. *Proc. Natl. Acad. Sci. U.S.A.* **2006**, *103*, 18928.
(38) Rhee, G.-Y.; Sokol, R. C.; Bethoney, C. M.; Cho, Y.-C.; Frohnhoefer, R. C.; Erkkila, T. Kinetics of polychlorinated biphenyl dechlorination and growth of dechlorinating microorganism. *Environ. Toxicol. Chem.* **2001**, *20*, 721−726.
(39) Burris, D. R.; Delcomyn, C. A.; Deng, B.; Buck, L. E.; Hatfield, K. Kinetics of tetrachloroethylene-reductive dechlorination catalyzed by vitamin B_{12}. *Environ. Toxicol. Chem.* **1998**, *17*, 1681−1688.
(40) Seshadri, R.; Adrian, L.; Fouts, D. E.; Eisen, J. A.; Phillippy, A. M.; Methe, B. A.; Ward, N. L.; Nelson, W. C.; Deboy, R. T.; Khouri, H. M.; Kolonay, J. F.; Dodson, R. J.; Daugherty, S. C.; Brinkac, L. M.; Sullivan, S. A.; Madupu, R.; Nelson, K. E.; Kang, K. H.; Impraim, M.; Tran, K.; Robinson, J. M.; Forberger, H. A.; Fraser, C. M.; Zinder, S. H.; Heidelberg, J. F. Genome sequence of the PCE-dechlorinating bacterium *Dehalococcoides ethenogenes*. *Science* **2005**, *307*, 105−108.
(41) Hölscher, T.; Krajmalnik-Brown, R.; Ritalahti, K. M.; von Wintzingerode, F.; Görisch, H.; Löffler, F. E.; Adrian, L. Multiple nonidentical reductive-dehalogenase-homologous genes are common in *Dehalococcoides*. *Appl. Environ. Microbiol.* **2004**, *70*, 5290−5297.
(42) Chow, W. L.; Cheng, D.; Wang, S.; He, J. Identification and transcriptional analysis of *trans*-DCE-producing reductive dehalogenases in *Dehalococcoides* species. *ISME J.* **2010**, *4*, 1020−1030.
(43) Cheng, D.; He, J. Isolation and characterization of "*Dehalococcoides*" sp. strain MB, which dechlorinates tetrachloroethene to *trans*-1,2-dichloroethene. *Appl. Environ. Microbiol.* **2009**, *75*, 5910−5918.
(44) van der Zaan, B.; Hannes, F.; Hoekstra, N.; Rijnaarts, H.; de Vos, W. M.; Smidt, H.; Gerritse, J. Correlation of *Dehalococcoides* 16S rRNA and chloroethene-reductive dehalogenase genes with geochemical conditions in chloroethene-contaminated groundwater. *Appl. Environ. Microbiol.* **2010**, *76*, 843−850.
(45) Gruber, K.; Puffer, B.; Kräutler, B. Vitamin B_{12}-derivatives-enzyme cofactors and ligands of proteins and nucleic acids. *Chem. Soc. Rev.* **2011**, *40*, 4346−4363.
(46) He, J.; Holmes, V. F.; Lee, P. K. H.; Alvarez-Cohen, L. Influence of vitamin B_{12} and cocultures on the growth of *Dehalococcoides* isolates in defined medium. *Appl. Environ. Microbiol.* **2007**, *73*, 2847−2853.
(47) Fennell, D. E.; Gossett, J. M.; Zinder, S. H. Comparison of butyric acid, ethanol, lactic acid, and propionic acid as hydrogen donors for the reductive dechlorination of tetrachloroethene. *Environ. Sci. Technol.* **1997**, *31*, 918−926.
(48) Tang, S.; Edwards, E. A. Identification of *Dehalobacter* reductive dehalogenases that catalyse dechlorination of chloroform, 1,1,1-trichloroethane and 1,1-dichloroethane. *Philos. Trans. R. Soc., B* **2013**, *368*, 20120318.
(49) Kublik, A.; Deobald, D.; Hartwig, S.; Schiffmann, C. L.; Andrades, A.; von Bergen, M.; Sawers, R. G.; Adrian, L. Identification of a multi-protein reductive dehalogenase complex in *Dehalococcoides mccartyistrain* strain CBDB1 suggests a protein-dependent respiratory electron transport chain obviating quinone involvement. *Environ. Microbiol.* **2016**, *18*, 3044−3056.
(50) Yan, J.; Rash, B. A.; Rainey, F. A.; Moe, W. M. Isolation of novel bacteria within the *Chloroflexi* capable of reductive dechlorination of 1,2,3-trichloropropane. *Environ. Microbiol.* **2009**, *11*, 833−843.
(51) Moe, W. M.; Yan, J.; Nobre, M. F.; da Costa, M. S.; Rainey, F. A. *Dehalogenimonas lykanthroporepellens* gen. nov., sp. nov., a reductively dehalogenating bacterium isolated from chlorinated solvent-contaminated groundwater. *Int. J. Syst. Evol. Microbiol.* **2009**, *59*, 2692−2697.
(52) Bowman, K. S.; Nobre, M. F.; da Costa, M. S.; Rainey, F. A.; Moe, W. M. *Dehalogenimonas alkenigignens* sp. nov., a chlorinated-alkane-dehalogenating bacterium isolated from groundwater. *Int. J. Syst. Evol. Microbiol.* **2013**, *63*, 1492−1498.
(53) Key, T. A.; Bowman, K. S.; Lee, I.; Chun, J.; Albuquerque, L.; da Costa, M. S.; Rainey, F. A.; Moe, W. M. *Dehalogenimonas formicexedens* sp. nov., a chlorinated alkane-respiring bacterium isolated from contaminated groundwater. *Int. J. Syst. Evol. Microbiol.* **2017**, *67*, 1366−1373.
(54) Werner, J. J.; Ptak, A. C.; Rahm, B. G.; Zhang, S.; Richardson, R. E. Absolute quantification of *Dehalococcoides* proteins: enzyme bioindicators of chlorinated ethene dehalorespiration. *Environ. Microbiol.* **2009**, *11*, 2687−2697.
(55) Kucharzyk, K. H.; Meisel, J. E.; Kara-Murdoch, F.; Murdoch, R. W.; Higgins, S. A.; Vainberg, S.; Bartling, C. M.; Mullins, L.; Hatzinger, P. B.; Löffler, F. E. Metagenome-guided proteomic quantification of reductive dehalogenases in the *Dehalococcoides mccartyi*-containing consortium SDC-9. *J. Proteome Res.* **2020**, *19*, 1812−1823.
(56) Maillard, J.; Schumacher, W.; Vazquez, F.; Regeard, C.; Hagen, W. R.; Holliger, C. Characterization of the corrinoid iron-sulfur protein tetrachloroethene reductive dehalogenase of *Dehalobacter restrictus*. *Appl. Environ. Microbiol.* **2003**, *69*, 4628−4638.
(57) Bommer, M.; Kunze, C.; Fesseler, J.; Schubert, T.; Diekert, G.; Dobbek, H. Structural basis for organohalide respiration. *Science* **2014**, *346*, 455−458.
(58) Yi, S.; Seth, E. C.; Men, Y.-J.; Stabler, S. P.; Allen, R. H.; Alvarez-Cohen, L.; Taga, M. E. Versatility in corrinoid salvaging and remodeling pathways supports corrinoid-dependent metabolism in *Dehalococcoides mccartyi*. *Appl. Environ. Microbiol.* **2012**, *78*, 7745−7752.

https://dx.doi.org/10.1021/acs.est.0c07354
Environ. Sci. Technol. 2021, 55, 4831−4841

(59) Shelton, A. N.; Seth, E. C.; Mok, K. C.; Han, A. W.; Jackson, S. N.; Haft, D. R.; Taga, M. E. Uneven distribution of cobamide biosynthesis and dependence in bacteria predicted by comparative genomics. *ISME J.* **2019**, *13*, 789−804.
(60) Helliwell, K. E.; Lawrence, A. D.; Holzer, A.; Kudahl, U. J.; Sasso, S.; Kräutler, B.; Scanlan, D. J.; Warren, M. J.; Smith, A. G. Cyanobacteria and eukaryotic algae use different chemical variants of vitamin B_{12}. *Curr. Biol.* **2016**, *26*, 999−1008.
(61) Sañudo-Wilhelmy, S. A.; Cutter, L. S.; Durazo, R.; Smail, E. A.; Gómez-Consarnau, L.; Webb, E. A.; Prokopenko, M. G.; Berelson, W. M.; Karl, D. M. Multiple B-vitamin depletion in large areas of the coastal ocean. *Proc. Natl. Acad. Sci. U.S.A.* **2012**, *109*, 14041−14045.
(62) Cadieux, N.; Bradbeer, C.; Reeger-Schneider, E.; Köster, W.; Mohanty, A. K.; Wiener, M. C.; Kadner, R. J. Identification of the periplasmic cobalamin-binding protein BtuF of *Escherichia coli*. *J. Bacteriol.* **2002**, *184*, 706−717.
(63) Lewinson, O.; Lee, A. T.; Locher, K. P.; Rees, D. C. A distinct mechanism for the ABC transporter BtuCD-BtuF revealed by the dynamics of complex formation. *Nat. Struct. Mol. Biol.* **2010**, *17*, 332−338.
(64) Men, Y.; Seth, E. C.; Yi, S.; Allen, R. H.; Taga, M. E.; Alvarez-Cohen, L. Sustainable growth of *Dehalococcoides mccartyi* 195 by corrinoid salvaging and remodeling in defined lactate-fermenting consortia. *Appl. Environ. Microbiol.* **2014**, *80*, 2133−2141.
(65) Men, Y.; Feil, H.; VerBerkmoes, N. C.; Shah, M. B.; Johnson, D. R.; Lee, P. K. H.; West, K. A.; Zinder, S. H.; Andersen, G. L.; Alvarez-Cohen, L. Sustainable syntrophic growth of *Dehalococcoides ethenogenes* strain 195 with *Desulfovibrio vulgaris* Hildenborough and *Methanobacterium congolense*: global transcriptomic and proteomic analyses. *ISME J.* **2012**, *6*, 410−421.
(66) Kruse, S.; Türkowsky, D.; Birkigt, J.; Matturro, B.; Franke, S.; Jehmlich, N.; von Bergen, M.; Westermann, M.; Rossetti, S.; Nijenhuis, I.; Adrian, L.; Diekert, G.; Goris, T. Interspecies metabolite transfer and aggregate formation in a co-culture of *Dehalococcoides* and *Sulfurospirillum* dehalogenating tetrachloroethene to ethene. *ISME J.* **2021**, DOI: 10.1038/s41396-020-00887-6. In press.
(67) Felchner-Zwirello, M.; Winter, J.; Gallert, C. Interspecies distances between propionic acid degraders and methanogens in syntrophic consortia for optimal hydrogen transfer. *Appl. Microbiol. Biotechnol.* **2013**, *97*, 9193−9205.
(68) Mao, X.; Stenuit, B.; Polasko, A.; Alvarez-Cohen, L. Efficient metabolic exchange and electron transfer within a syntrophic trichloroethene-degrading coculture of *Dehalococcoides mccartyi* 195 and *Syntrophomonas wolfei*. *Appl. Environ. Microbiol.* **2015**, *81*, 2015−2024.
(69) Chau, A. T. T.; Lee, M.; Adrian, L.; Manefield, M. J. Syntrophic partners enhance growth and respiratory dehalogenation of hexachlorobenzene by *Dehalococcoides mccartyi* strain CBDB1. *Front. Microbiol.* **2018**, *9*, 1927.

https://dx.doi.org/10.1021/acs.est.0c07354
Environ. Sci. Technol. 2021, 55, 4831−4841